

**THE HP<sup>3</sup> RADIOMETER FOR THE INSIGHT MISSION.** N. Mueller<sup>1</sup>, E. Kopp<sup>1</sup>, I. Walter<sup>1</sup>, M. Grott<sup>1</sup>, J. Knollenberg<sup>1</sup>, M. Siegler<sup>2</sup>, S. Smrekar<sup>2</sup>, F. Hänschke<sup>3</sup>, E. Kessler<sup>3</sup>, T. Spohn<sup>1</sup>, <sup>1</sup>German Aerospace Center (DLR), Rutherfordstr. 2, 12489 Berlin, Germany (nils.mueller@dlr.de), <sup>2</sup>Jet Propulsion Laboratory (JPL), 4800 Oak Grove Drive, La Cañada Flintridge, CA 91011, USA. <sup>3</sup>Leibniz Institute of Photonic Technology e.V. (IPHT), PF 100239, 07702 Jena, Germany

**Introduction:** The NASA mission InSight is scheduled to land on Mars in 2016. The mission is designed to operate for at least one Martian year on the surface. The German Aerospace Center (DLR) provides the Heatflow and Physical Properties Package (HP<sup>3</sup>), designed to estimate the planetary heat flow by deploying an instrumented tether 3 - 5 m into the Martian regolith using a self-penetrating probe, called the mole. Subsurface temperature gradient is measured by temperature sensors on the tether and thermal conductivity is measured at various depths by heating the mole and recording the self-heating curve [1].

The subsurface temperature gradient imposed by the planetary heat flow is disturbed by diurnal, annual and interannual surface temperature variation. If the tether is deployed down to 3m depths and measures for one Martian year, the geothermal gradient can be separated from the diurnal and annual heat waves with sufficient accuracy while interannual temperature variations are not expected to be significant [2].

For the cases that the tether cannot be deployed below 3 m, the instrument fails before operating for one year, or interannual temperature variations are larger than expected, a radiometer measuring the surface brightness temperature at fixed spots in the vicinity of the lander was added to the package in order to have a constraint on the surface temperature forcing. Measurement of the surface temperature allows to disentangle the contributions of the diurnal and annual heat waves from the geothermal gradient.

**Objectives:** The radiometer aims at detecting changes in the surface properties caused by the rocket assisted landing and subsequent resettling of dust. Furthermore the effect of the lander shadow and thermal radiation on the surface temperature will be studied. Lastly, the surface brightness temperature provides a link between the in-situ subsurface temperature measurements by InSight and the long duration observation of surface temperature by remote sensing (Viking orbiter IRTM, Mars Global Surveyor TES, Mars Odyssey THEMIS). An additional possible analysis is the study of thermal inertia of the measured spots over the course of one year.

**Design:** The design has heritage from MUPUS-TM on the comet lander Philae of the Rosetta mission (ESA) [3], the MERTIS - radiometer on the Mercury orbiter Bepi Colombo (ESA) [4], MARA on the asteroid hopper Mascot (DLR) [5] to be deployed during

the Hayabusa 2 mission (JAXA). The design uses thermopile sensors (by IPHT) to measure the radiative heat exchange between the observed surface and the instrument, which is kept at a stable temperature. Six thermopile sensors are housed in an aluminum body, aligned to observe two spots on the surface with three sensors each. The sensors include spectral filters transparent to different ranges longwards of 6  $\mu\text{m}$ . To provide protection against dust and debris during landing a movable dust cover is included. The dust cover temperature can be controlled and will be used to recalibrate the instrument during flight and the landed mission.

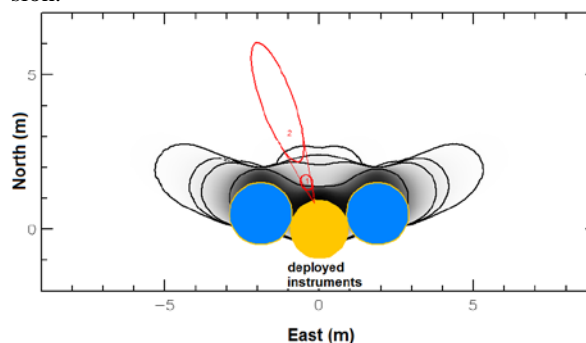


**Figure 1:** Top view of lander outline (yellow and blue), its shadow as loss of insolation integrated over the day of northern winter solstice (grey) and the radiometer FOVs (red).

**Field of View:** The radiometer is mounted below the lander deck and observes in two 20° cones towards NNW of the InSight lander, facing away from the instrument deployment workspace south of the lander to avoid hardware in the field of view. Fig. 1 shows the expected orientation of lander and solar panels (yellow and blue) FOVs (red) and approximate effect of shadowing (greyscale) for the day of the northern winter solstice assuming a landing site at 4° N. The outer field of view avoids most of the shadow. For at least half of the year the inner FOV is out of the shadow as well, which then can be compared to the outer FOV to study the effect of lander thermal radiation and obscuration of cold sky. Most of both fields of view can be imaged by the camera mounted on the instrument deployment arm.

**Spectral bands:** Two of the spectral filters are identical to those of the REMS-GTS radiometer on MSL (NASA) [6]. The third REMS-GTS filter targets the CO<sub>2</sub> absorption band at 15  $\mu\text{m}$  to measure atmos-

pheric temperature. For InSight, the atmospheric path is shorter and therefore there is less sensitivity to atmospheric temperature. The third filter will instead be either a bandpass 7.8-8.6  $\mu\text{m}$  allowing us a better deconvolution into different brightness temperature components within the FOV or a longpass opening at 6  $\mu\text{m}$  which provides superior temperature resolution (Fig. 2).

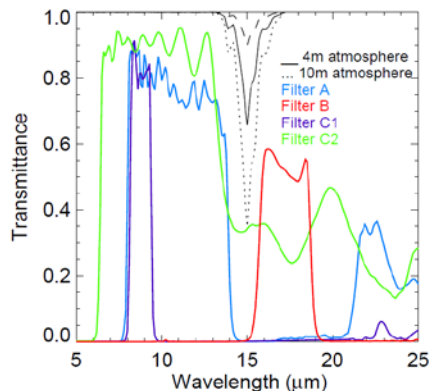


**Figure 2:** Transmittance of sensor filter windows and the martian atmosphere for different optical path lengths.

**Operations and performance:** To improve the accuracy and precision of measurements the instrumental temperature is stabilized. The design uses only heaters for stabilization therefore the instrument temperature needs to be kept above equilibrium temperature, mostly determined by atmospheric temperature.

There are two main modes of observation. At least once every  $15^\circ$  of  $L_s$  the radiometer measures surface brightness temperature hourly in order to determine the shape of the diurnal cycle. On all other sols (power and data rate permitting) the radiometer measures only 4 times per sol, at 2/5 am/pm local solar time, i.e. synchronized with MGS and Mars Odyssey observations. Fig. 3 shows a simulated measurement of the surface temperature modeled using the KRC model [7].

Relevant for constraining the variation of the heat flow at depths greater than a few centimeters is the variation of daily average temperature with season. Since the radiometer measures brightness temperature, the derived temperature includes an error from the unknown emissivity. Mini-TES measurements on the Mars Exploration rovers [eg. 8] show that the emissivity can be expected to fall within 2% of 0.97 in the 8-14  $\mu\text{m}$  range (Filter A).

The error due to emissivity is proportional to the measured net heat flux between instrument and surface and, thus, is larger for larger differences between instrument and surface temperatures. Therefore, the temperature setpoint for night operations is chosen as the

minimum operating temperature of the radiometer electronics (240K).

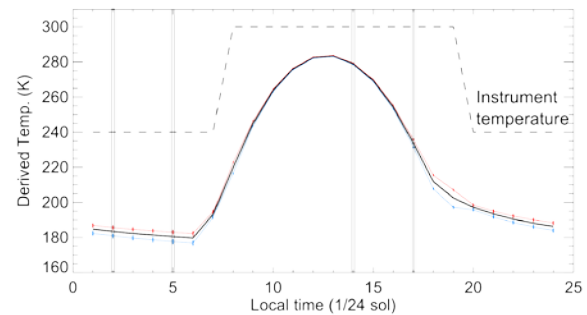


**Figure 3 :** Operational profile and modeled measurements for one sol. See text for more details.

Fig. 3 shows a profile of derived temperatures assuming correct (black) and 2% incorrect emissivities (blue and red). The expected instrumental measurement error is  $< 2\text{K}$  at 170K surface temperature and shown for as error bars for the red and blue plot at each  $1/24^{\text{th}}$  of a sol..

Together the systematic bias from the unknown emissivity and the measurements uncertainty are sufficiently small to constrain the variation of subsurface heatflow at 2m depth to within  $3\text{mW/m}^2$ , assuming that the thermal conductivity is known from the HP<sup>3</sup> mole measurements and within the expected range [2].

## References:

- [1] Spohn et al, (2014), Measuring the Martian Heat Flow using the Heat Flow and Physical Properties Package (HP<sup>3</sup>). abstract at this conference
- [2] Grott, M., et al. (2007). JGR, 112, E09004, doi:10.1029/2007JE002905
- [3] Spohn et al. (2007) Space Sci. Rev., 128: 339–362. DOI: 10.1007/s11214-006-9081-2
- [4] Walter, I. et al. ; (2006) Proc. SPIE 6297, IR. Spaceborne Rem. Sens. XIV, doi:10.1117/12.679481
- [5] Grott et al. (2013), 44th LPSC. LPI Contr. No. 1719, p.1586
- [6] Gomez-Elvira et al. (2012): Space Sci Rev., 170:583–640. DOI 10.1007/s11214-012-9921-1
- [7] Kieffer, H. H. (2013), JGR-Planets, 118, 451–470, doi:10.1029/2012JE004164.
- [8] Ruff et al. (2006);, JGR, 111, E12S18, doi:10.1029/2006JE002747